HSM2021-2021134

EFFECTS OF CONSTITUTIVE MODEL PARAMETERS ON FINITE ELEMENT SIMULATION PROCESS FOR HARD MILLING OF AISI H13 STEEL

S. Zhang [ab*], B. Li [ab], J. Li [ab], J. Man [ab]

[a] Shandong University, School of Mechanical Engineering, Key Laboratory of High Efficiency and Clean Mechanical Manufacture of Ministry of Education, Jinan, China

[b] Shandong University, Key National Demonstration Center for Experimental Mechanical Engineering Education, Jinan, China

[*] Corresponding author/E-mail: zhangsong@sdu.edu.cn

Abstract

During the metal cutting process, finite element (FE) simulation has been acknowledged as an efficient way to provide designers more in-depth understanding. Furthermore, constitutive model parameters of the experimental material play a crucial role in determining the accuracy of FE simulation results. In this study, three different sets of Johnson-Cook (J-C) constitutive model parameters (*A*, *B*, *n*, *c*, and *m*) in literature were chosen to investigate the influence on numerical modeling for hard milling of AISI H13 steel. Hard milling experiment was conducted to compare the simulation results obtained by varying constitutive model parameters concerning chip morphology, cutting force, and cutting temperature. The parameter A has a significant influence on chip morphology and cutting force compared to other parameters, while the parameter m shows little impact on cutting temperature variation. The comparison between experimental and predicted results indicates that the considered machining outputs are sensitive to adopted constitutive model parameters, in particular the chip morphology. Based on the analysis, it can be confirmed that constitutive model parameters calibration in advance is a necessary procedure before applying it to metal machining simulation.

Keywords:

Constitutive model parameters; FE simulation process; Hard milling; AISI H13 steel

1 INTRODUCTION

With the advancement of machining tools and cutting tools, metal machining has also stepped a great stride towards achieving high productivity with the adoption of aggressive cutting parameters. Under the aggressive cutting conditions, the metal-physical phenomena appeared in cutting deformation zones due to the coupled action of large strain, stress, and high temperature [1]. Furthermore, a better understanding of meta-physical behavior in the metal cutting process is of great importance for cutting parameter optimization and surface quality improvement [2]. However, in the practical cutting operation, it is hard to measure the shear strain, stress, and cutting temperature, not to mention the

microstructure evolution. Thanks to the great progress in finite element modeling, it is a powerful tool that provides an efficient method to simulate the actual cutting process in a quite similar environment by many researchers. Through cutting simulation, the distribution of cutting temperature, shear strain, and stress can be obtained simultaneously, which provides great help for the in-depth understanding of machining behavior and reveal the underlying mechanism of chip formation [3-5].

It is well-known that the materials constitutive model plays a key role in determining the accuracy of the prediction results. The common material constitutive models are including but are not limited to Johnson-Cook (J-C), Zerilli–Armstrong, and Power-Law et al. However, the J-C model is the most widely used constitutive model to describe the material flow behavior during metal cutting with satisfactory simulation results in comparison to experimental data [6-8]. Therefore, a set of reliable J-C parameters is the prerequisite before performing finite element simulation [9]. However, most of the J-C parameters are obtained through conducting split Hopkinson press bar (SHPB) experiments to approach as close as too high strain rate occurred in high-speed machining [10]. Even though the strain rate in metal cutting can reach up to 10^5 s^{-1} [11], the SHPB experiments are outside this range. It is assumed that the J-C parameters obtained under that condition are hard to describe the material flow behavior accurately, even in face of the same material. Consequently, the required calibration and modification procedures for J-C constitutive model parameters with the assistance of various methods are inevitable [12-14].

Finite element modeling of material behavior in the metal cutting process such as hardened AISI H13 steel is of significance in studying hard machining. AISI H13 steel is a hot work die steel, which is widely used in die-cast and mold manufacture due to its outstanding thermomechanical properties [15]. AISI H13 steel is classified as hard-to-machining material due to its high hardness and strength and generates serrated chips in the cutting process. Several scholars have attempted finite element modeling of the AISI H13 cutting process

using different constitutive model parameters [16-19]. However, as far as the constitutive model is concerned, quite limited researchers conduct the study on the sensitivity of the constitutive model parameter, particularly AISI H13 steel.

In this present study, three different sets of Johnson-Cook (J-C) constitutive model parameters in literature were chosen to investigate the influence on simulated chip morphology, cutting force, and temperature in the hard milling of AISI H13 steel. Hard milling experiment was conducted to compare the simulation results obtained by varying constitutive model constants correspondingly. Furthermore, the sensitivity of the constitutive model on simulation results is analyzed.

2 EXPERIMENTAL PROCEDURE

Hard milling tests were carried out on hardened AISI H13 steel block with a hardness of 50 ± 2 HRC using a DAEWOO CNC vertical machine. Coated Seco tool (XOMXO090308TR-M08, MP1500) was chosen and mechanically mounted on a Seco tool holder (R217.69-2020.0-09-3A N) providing a rake angle +10° and clearance angle +15°, respectively. The workpiece was mounted on a Kistler 9257B piezoelectric dynamometer, which was used for cutting force measurement. The produced chip was mounted and polished for chip morphology observation under SEM. The cutting condition is v_c = 300 m/min, f_z = 0.2 mm/tooth, a_e = a_p = 2.0 mm. A detailed machining experimental setup is shown in Fig. 1.
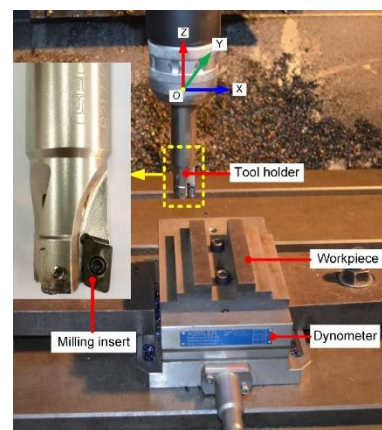

Fig. 1: Experimental setup.

3 J-C CONSTITUTIVE CONSTANT AND FINITE ELEMENT MODEL

The commonly used Johnson-cook constitutive equation is listed as follows [20]:

$$\sigma = \left(A + B\varepsilon^n\right)\left[1 + C\left(\frac{\dot{\varepsilon}}{\dot{\varepsilon}_0}\right)\right]\left[1 - \left(\frac{T - T_r}{T_m - T_r}\right)^m\right] \quad (1)$$

Where σ is the equivalent flow stress, constants A, B, n, C and m represent initial yield strength, strain hardening constant, strain hardening exponent, strain rate sensitivity, and thermal softening coefficient, respectively. T is the current temperature, T_m is the melting temperature, and T_r is the transition temperature. Table 1 lists three sets of J-C constants adopted by several researchers. The material constant sets M1 and M3 are identified through experimental results under a wide range of strain rates and temperatures, while M2 is identified through regression analysis. The related thermal and mechanical properties of AISI H13 steel can also be found in the corresponding reference.

Tab. 1: J-C constants of AISI H13 steel in literature.

	A (MPa)	B (MPa)	n	C	m	$\dot{\varepsilon}$(s⁻¹)	Hardness	Ref.
M1	674.8	239.2	0.44	0.056	2.7	-	50 HRC	[16]
M2	908.54	321.39	0.278	0.028	1.18	1.0	52 HRC	[17, 18]
M3	1695	1088	0.6272	0.0048	0.52	0.001	50 HRC	[19]

Element type CPE4RT was assigned to both workpiece and tool. The left, right, and bottom boundaries of the workpiece were fully constrained, and the cutting tool was merely allowed to rotate along the assigned central point. The cutting tool is regarded as a rigid body for simplicity. The workpiece and cutting tool were respectively subdivided into 78507 elements and 156 elements. Coulomb's friction law was applied to describe the friction behavior between the workpiece and cutting tool and the coefficient of friction was set to μ=0.3. A thermo-mechanical coupled FE analysis under plain-strain assumption was conducted. When conducting the FE simulation for AISI H13 steel, the input parameters are all kept the same except the J-C model constants cited from Ref. [10-13].
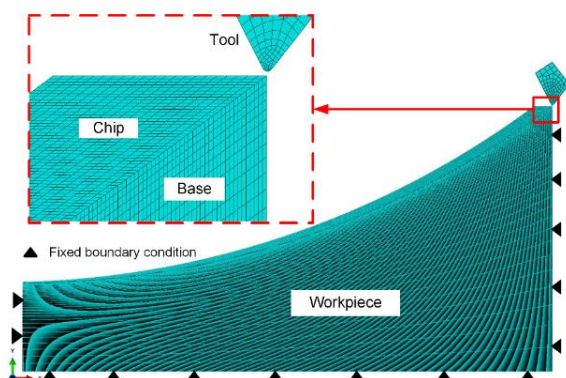

Fig.2: Established FE cutting simulation model for AISI H13 steel

4 RESULTS AND DISCUSSION

The predicted distribution of temperature and equivalent plastic strain under different J-C model parameters are listed in Table 2. The simulated results in terms of chip morphology are in different shapes. When adopting the model constants M3, the chip morphology is serrated chip, while the produced chip demonstrates continuous chip when using the model M1 and M2. It should be highlighted that the periodical shear localization is about to generate showing the initiation, which is believed to be the precursor of the adiabatic shear band. As far as the cutting temperature is concerned, the temperature distribution between tool rake face and chip back surface is more severe and the distribution length with a high-temperature value is longer with M3. On the contrary, the high-temperature region under M1 and M2 between the tool-chip contact surface is localized without showing an extended length along the direction of the chip flows out. Materials ahead of the tool tip are inclined to yield under a large thermal softening coefficient m (M1) with less mechanical energy input, while materials with higher A and B values require more energy to reach the shear flow stress. The extended high temperature distribution along the chip back surface under M3 is a good reflection of a small value of m. On the other

hand, large *m* tends to reduce the degree of shear strain between two segments, which verifies the difficulty in serrated chip formation [20]. In a conclusion, the formation of the serrated chip tends to aggravate the friction behavior between tool rake face and chip. After all, the periodical generation of serrated chips will induce the fluctuation of cutting force and cutting instability [21, 22], which eventually causes a

much worse condition. Furthermore, the shear localization with large strain in the serrated chip is mainly located between two segments for M3. Comparatively, the shear localization is weak in the continuous chip for M1 and M2. Instead, the whole continuous chip is subjected to shear strain while in a small value.
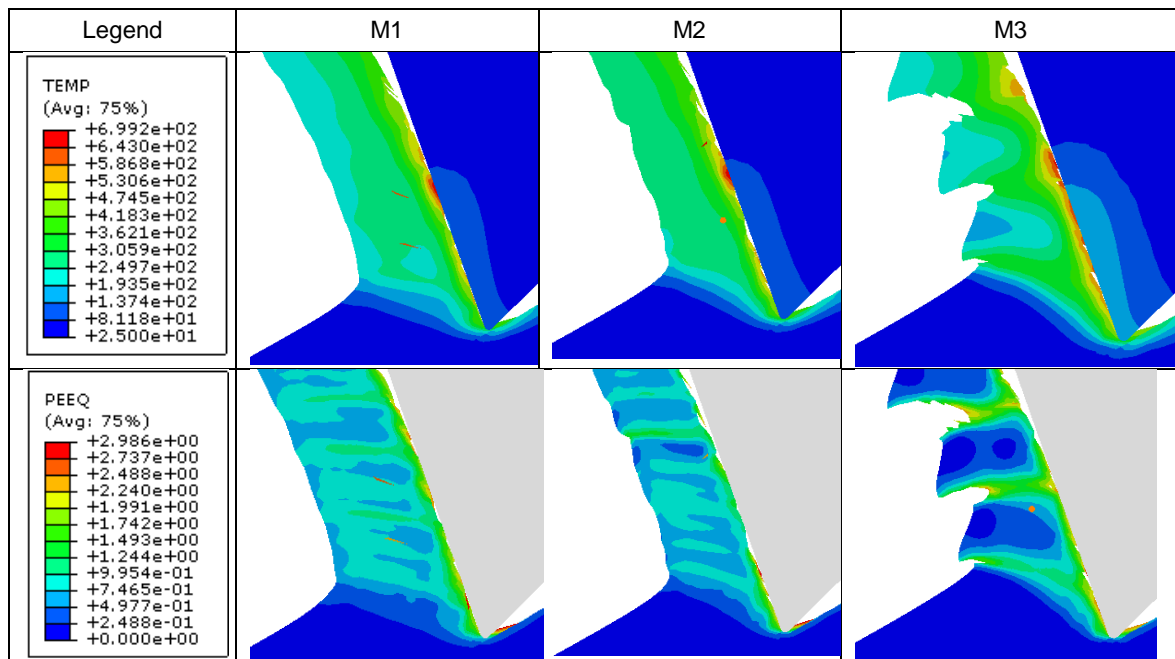

Fig. 3: Predicted results by varying J-C model parameters (step = 80).

Fig. 4 plots the predicted cutting force in *x* and *y* directions by varying the J-C parameters. Although the cutting force fluctuates obviously during one cutting cycle, it appears that the cutting force overall increases first and then gradually reduces with the uncut chip thickness becomes thinner. The increasing cutting force at the very beginning is mainly attributed to the increased cutting-edge engagement with the workpiece as the tool progresses. The maximum cutting force is observed around cutting time 0.2×10^{-3} s due to the full engagement of the cutting insert. When comparing the cutting forces, it can be found that they are very similar between M1 and M2 regarding

variation trend and magnitude, while a little higher value and fluctuation amplitude are demonstrated with M3. For J-C model parameters, *A*, *B* and *n* respectively denote material yield strength, hardening strain factor, and strain hardening exponent, which can significantly affect the cutting force during the metal cutting process. Therefore, *A*, *B,* and *n* in M3 show larger values in comparison to those in M1 and M2 eventually lead to higher cutting forces. Moreover, a larger thermal softening factor *m* indicates that the material is more prone to yield, which reflects in the lower cutting force.
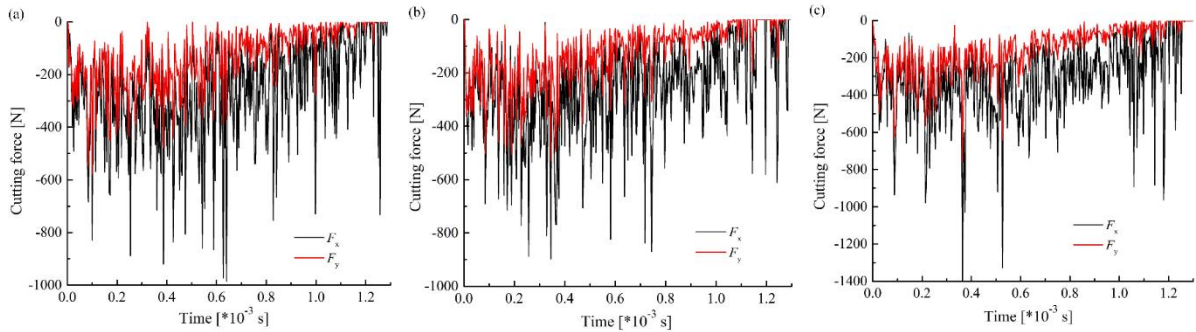
Fig. 4: Predicted cutting forces: (a) M1; (b) M2; (c) M3.

Generally, accurate prediction of chip morphology and cutting force is considered as an indicator to evaluate the accuracy of constitutive models in FE modeling [23]. Fig. 5 shows the experimentally obtained serrated chip. The chip morphology is quite different from the predicted chip morphology with J-C model parameters M1 and M2, which exhibits continuous uniform chip morphology. Regarding M3, the simulated serrated chip is similar to the experimental chip morphology overall. It can be confirmed that using different material constitutive model parameters eventually leads to different chip morphology. According to Ref. [24], it was reported that a larger A and B promote the
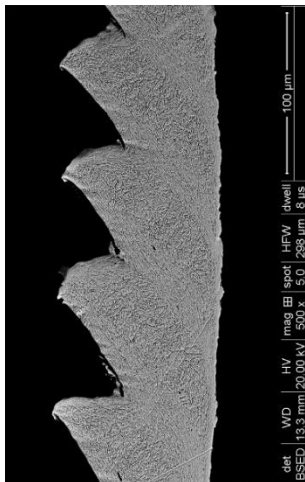
serration formation. More in detail, the serrated chip with segmentation has a significant influence on cutting force, chip–tool interface temperature, and the dynamic behavior of the whole cutting system [25]. As far as the cutting force is concerned, the variation trend between measurement and prediction with various model parameters is in good agreement, which increases firstly and then decreases gradually to zero. In terms of cutting force value, the predicted value with M3 is closer to the experimental results compared to M1 and M2. This can be reflected in the J-C model parameters with a higher *A* and *B* value but a small *m* (thermal softening) for M3.
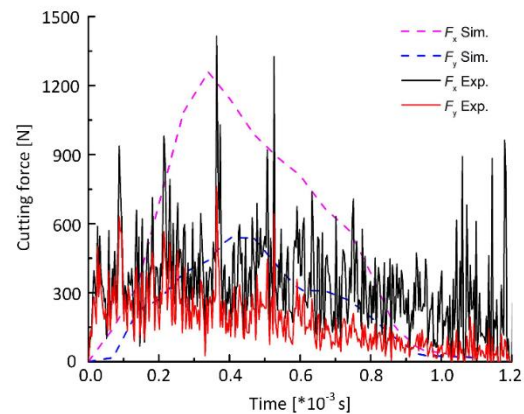

Fig. 5: Experimental chip morphology.

Fig. 6: Experimentally measured cutting forces.

5 CONCLUSIONS

Different J-C material constitutive model parameters were adopted to investigate the influence on chip morphology and cutting forces in finite element modeling of cutting of AISI H13 steel. The main conclusions can be summarized as follows:

• Different J-C constitutive model parameters are obtained in the literature for AISI H13 steel ending with quite different predicted chip morphology.

• The J-C model parameters provided by Lu provide a relatively accurate prediction for serrated chip and cutting forces compared with experimental results.

• J-C model parameters are mostly obtained through tests, which should highlight that model calibration before cutting simulation is a necessary procedure.

To guarantee model accuracy, the next steps to identify J-C constitutive model constants for different materials should consider combining the SHPB tests and machining tests. The further improvements aim to correctly describe the material shear behavior encountered in high-speed machining processes under super high strain rate and high temperature as well as to facilitate the applicability of the cutting simulation in industries with little economical effort and enhancement of surface quality.

ACKNOWLEDGMENT

REFERENCES

[Astakhov VP 2004] Astakhov, V.P., et al. The assessment of plastic deformation in metal cutting. Journal of Materials Processing Technology 2004;146[2], 193-202.

[Jang 1992] Jang, D.Y., and Seireg, A. Machining parameter optimization for specified surface conditions. Journal of Manufacturing Science and Engineering, 1992, 254-257

[Caruso 2020] Caruso, S., et al. Finite Element Modeling of Microstructural Changes in Hard Machining of SAE 8620. Applied Sciences, 2020,10(1),121.

[Gok 2017] Gok, K., et al. Three-dimensional finite element modeling of effect on the cutting forces of rake angle and approach angle in milling. ARCHIVE Proceedings of the Institution of Mechanical Engineers Part E Journal of Process Mechanical Engineering, 2017, 231(2), 83-88.

[Oezel 2017] Oezel, T., Olleak, A., and Thepsonthi, T. Micro milling of titanium alloy Ti-6Al-4V: 3-D finite element modeling for prediction of chip flow and burr formation. Production Engineering, 2017, 11(4-5), 435-444.

[Ducobu 2017] Ducobu, F., Rivière-Lorphèvre, E., and Filippi, E. On the importance of the choice of the parameters of the Johnson-Cook constitutive model and their influence on the results of a Ti6Al4V orthogonal cutting model. International Journal of Mechanical Sciences, 2017, 122, 143-155.

[Dodla 2021] Dodla S., Idnani,K., and Katyal A. (2021) Finite element machining simulations of aerospace materials. Materials Today: Proceedings, 46(2), 991-998.

[Hasa 2020] Hasa B., et al. (2020) Investigation of process parameters in orthogonal cutting using finite element approaches. Heliyon, 6(11), 1-10.

[Timothy 2021] Timothy No A., et al. (2021) Propagation of Johnson-Cook flow stress model uncertainty to milling force uncertainty using finite element analysis and time domain simulation. Procedia Manufacturing, 53, 223-235.

[Wang 2016] Wang, C., et al. Modeling and simulation of the high-speed milling of hardened steel SKD11 (62 HRC) based on SHPB technology. International Journal of Machine Tools & Manufacture, 2016, 108, 13-26.

[Johansson 2016] Johansson, J., et al. Microstructural examination of shear localisation during high strain rate deformation of alloy 718. Materials Science and Engineering A. 2016, 662, 363-372.

[Mg 2021] Mg A., et al. (2021) Analysis of two parameter identification methods for original and modified johnson-cook fracture strains, including numerical comparison and validation of a new blue-brittle dependent fracture model for free-cutting steel 50sib8. Theoretical and Applied Fracture Mechanics, 112, 102905.

[Bergs 2020] Bergs T., et al. (2020) Determination of johnson-cook material model parameters for AISI 1045 from orthogonal cutting tests using the downhill-simplex algorithm. Procedia Manufacturing, 48, 541-552.

[Li 2021] Li S., et al. (2021) Optimization of milling aluminum alloy 6061-t6 using modified johnson-cook

model. Simulation Modelling Practice and Theory, 111(9-12), 102330.

[Mutlu 2013] Mutlu, I., Oktay, E., and Ekinci, S. Characterization of microstructure of H13 tool steel using ultrasonic measurements. Russian Journal of Nondestructive Testing, 2013, 49, 112–120.

[Umer 2012] Umer, U. High-speed turning of H-13 tool steel using ceramics and PCBN. Journal of Materials Engineering & Performance, 2012, 21(9), 1857-1861.

[Yan 2005] Yan, H., Hua, J., and Shivpuri, R. Numerical simulation of finish hard turning for AISI H13 die steel. Science & Technology of Advanced Materials, 2005, 6(5), 540-547.

[Yan 2007] Yan, H., Hua, J., and Shivpuri, R. Flow stress of AISI H13 die steel in hard machining. Materials & Design, 2007, 28(1), 272-277.

[Lu 2008] Lu, S., and He, N. Experimental investigation of the dynamic behavior of hardened steel in high strain rate and parameter fitting of constitutive equation. China Mechanical Engineering, 2008, 19, 2382-2385.

[Arrazola 2010] Arrazola, P.J., Barbero, O., and Urresti, I. (2010) Influence of material parameters on serrated chip prediction in finite element modeling of chip formation process. International Journal of Material Forming, 3(1 Supplement), 519-522.

[Zhang 2013] Zhang, S., et al. Saw-tooth chip formation and its effect on cutting force fluctuation in turning of Inconel 718. International Journal of Precision Engineering & Manufacturing, 2013, 14(6), 957-963.

[Yadav 2019] Yadav, S., Feng, G., and Sagapuram, D. Dynamics of shear band instabilities in cutting of metals. CIRP Annals, 2019, 68(1), 45-48.

[Zhang 2014] Zhang, X.P., Shivpuri, R., and Srivastava, A.K. Role of phase transformation in chip segmentation during high-speed machining of dual phase titanium alloys. Journal of Materials Processing Technology, 2014, 214(12), 3048-66.

[Arrazola 2010] Arrazola, P.J., Barbero, O., and Urresti, I. Influence of material parameters on serrated chip prediction in finite element modeling of chip formation process. International Journal of Material Forming, 2010, 3(1), 519-522.

[Wang 2014] Wang, C., et al. Research on the chip formation mechanism during the high-speed milling of hardened steel. International Journal of Machine Tools and Manufacture, 2014, 79, 31-48.